OITAF
Bozen/Bolzano
Congress 2017

Cable ropeway simulation: computation and visualization of complex mechanical systems

M. Wenin, M. Irschara, S. Obexer, M. L. Bertotti and G. Modanese

Abstract

In this contribution we present results of computation and visualization of the mechanics of ropeways, in particular obtained over the last few years from our group of R&D. An example of a fix anchored cable, two supports and a quasi-static moving point load is discussed. Quantities as the space-resolved cable tension, the dissipated energy due to friction of the moving cable on the supports and oscillations of the point load are computed.

Introduction

The simulation of complex structures in engineering, the study of the behavior under different loading cases, the dynamical response of time-dependent external forces etc. is an important task in the practical construction process aimed in particular at cost reduction. A large class of practical problems in general mechanical and electrical or thermal engineering is described by partial differential equations including boundary/initial conditions and well established Finite Element Solvers exist (see for instance the MATLAB documentation for FEM, for an introduction in the mathematical foundations [1, 2]).

Yet in the field of ropeways only a few simulation programs are in use, because the market is small (compared with automotive industry) and the gap from academic investigations to the engineering offices seems large [3, 4]. Nevertheless the computer power grows rapidly and the possibilities for simulations and visualizations/sonifications achieved a high level [5, 6]. Here we show that the visualization of many physical properties can help the engineer in the construction phase and in the description of the physics of the plant both digitally and on paper.

Quasi-static approach

Within a quasi-static approach one assumes that all components of the mechanical system move with infinitely slow velocity. This not only implies neglecting inertial effects of accelerated masses, but also disregarding the initial conditions of the system. So the state of the ropeway at a time t does not depend on the past. For example: when a ropeway car moves from valley to a point with horizontal coordinate x_Z, the state of the system (all mechanical quantities as cable configurations, support forces etc.) is the same as when the car is coming from the mountain side. Both states are indistinguishable from mechanical point of view (one can compare this strategy with the adiabatic processes in thermodynamics). This is the reason why the quasi-static approach in practice is an excellent method to obtain characteristic numbers of the ropeway [7, 8]. The degrees of freedom to describe the state of the system and as a consequence the computational effort are reduced drastically. Additionally one can build upon such a computation different models or strategies to improve the results regarding friction resistances of the cables on the supports or mechanical effects of wind etc. However true time-dependent problems obviously are not exactly available by a quasi-static approximation [9,10]. In our approach we use the ideal, frictionless system as the zeroth order. In this state all parameters are uniquely defined and computable. Next, we compute the differences of the cable tension using the empty cable configuration and the charged cable configuration. If the difference is larger than the static friction, the cable moves and the dynamic friction is added to the cable tension. This procedure is obviously an approximation, but it avoids the naive addition of all friction resistances on all supports,

which in the presence of many supports leads to unphysical high cable tensions. As many practical applications have shown, a quite realistic estimation of the support cable tension is possible. A few words are in order about the role of the hauling cable. We use the approximation that the hauling cable at the point load position acts under an angle $\psi = (\alpha_+ + \alpha_-) / 2$, where $\alpha_{+/-}$ are the support cable angles at the point load [7]. We need these self-consistently computed angles to close the system of equations, when we determine the equilibrium cable configuration. This approach allows a decoupling of support- and hauling cable computation. Here we do not recall further standard results concerning the hauling cable.

Numerical example

We present here some numerical results (all results presented here are obtained with the help of the simulation program *Rope-E*, written in MATLAB), obtained by a quasi-static approach, using the ``elastic'' catenary. The example was chosen to show the visualization capabilities and to make interesting details visible. We restrict the discussion to some important features of the system. The table shows the coordinates of the plant, the linear mass density (tension-less, at a certain reference temperature) is ρ_L = 12 kg/m, the metallic cross section A = 1400 mm², the isothermal modulus of elasticity (assumed as temperature-independent) E = 160 kN/mm² and the mass of the point load m = 5000 kg respectively. For the cable force in the valley station at T_{ref} = 10 °C we set F_0 = 400 kN. The cable is held fixed at the endpoints. All presented results are based on a track-discretization with 200 points, giving a mean grid-width of 12.5 m.

Anchor. / sup. No.	Vall.	1	2	Mount.
X – coord. [m]	0	100	1000	2500
Y – coord. [m]	0	90	510	800

Let us discuss the figures: Fig. 1 shows the empty support cable and the positions of the supports. The lower part gives the midspan catenary sag for three different temperatures, where the maximum difference is in accordance with the CEN-standard equal ΔT = 60 °C. Fig. 2 is a collection of important physical quantities: The Upper left panel shows the cable tension $F(x , x_Z)$ as a function of position x and point load position x_Z, assuming no friction resistance on the supports. This plot gives a complete information of the tension for all (i.e. 200) positions for the frictionless gliding cable, when the point load moves infinitely slow (no retardation effects); it represents a tension landscape. The corresponding strain is also shown in the upper right panel. In the left lower panel we have plotted the maximum cable tension, which we can find by a scan of all values within the tension landscape. A continuous relationship arises for $F_{max}(x , x_Z)$; however when we include the friction resistance on the supports, this relation shows steps, originating from the step-like behavior of the cable/support friction interaction model of our approach. The detailed tension landscape for this situation is given in Fig. 4. The elastic lengthening of the cable is shown in the right lower panel of Fig. 2. All quantities are strongly temperature dependent. Fig. 3 shows the displacement of the support cable on the supports, when the position of the point load varies. Using the normal forces and the dynamic friction coefficient, we are able to estimate the friction losses. As the computations demonstrate, the values depend strongly on the cable tensions F_0, whereas the temperature dependence is weak (not shown here). Fig. 4 is devoted to the visualization of the support cable tension. The upper plots show a translation of tensions into

colors to make clearly visible the cable tension for an arbitrary point load position at any position. The lower contour plot provides, as we said before, the essence of the support cable computation, the correction of the tension landscape from Fig. 2 by the support friction. We extract from this huge table of tensions the extreme values, which are relevant for the engineer.

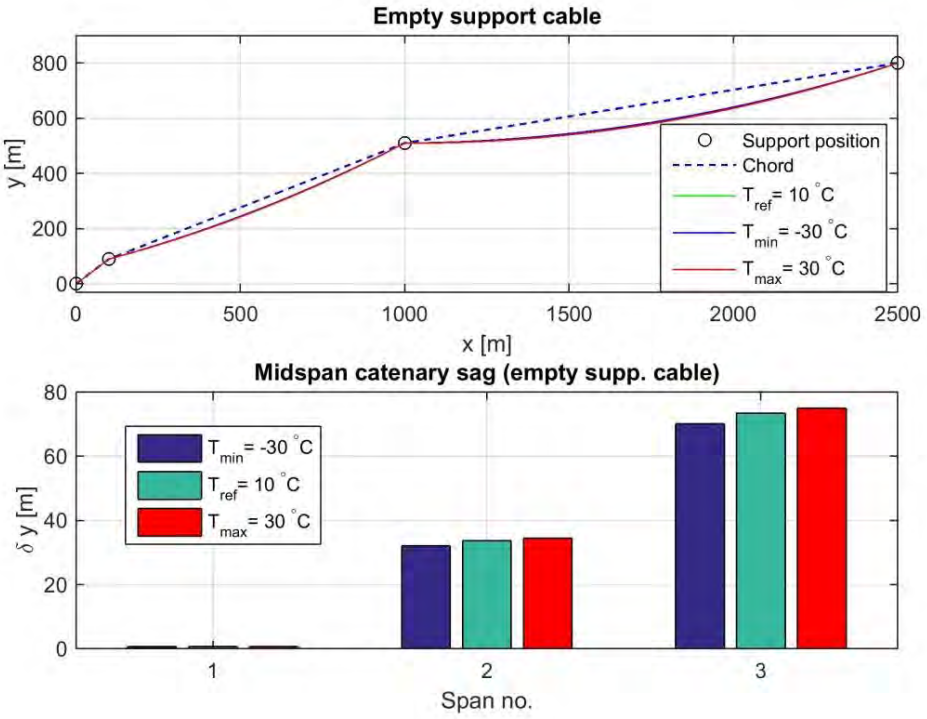

Fig. 1: *Support positions and empty support cable to give an impression of the model ropeway considered in this work. The lower histogram shows the midspan catenary sag for three different temperatures. The cable is fix anchored at the ends of the line.*

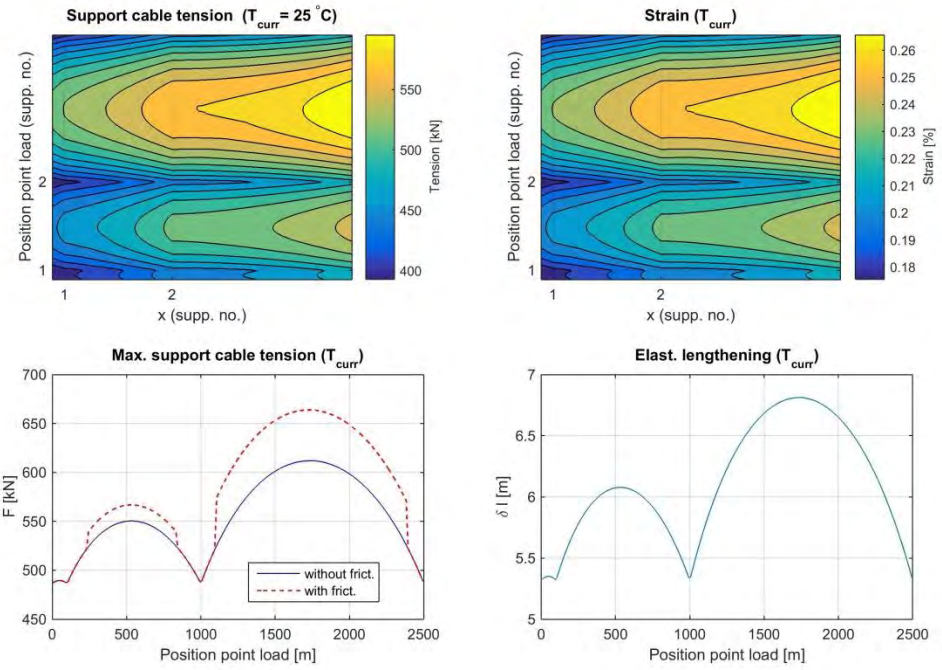

Fig. 2: *Data for the support cable: cable tension as a function of x (horizontal) and point load position x_Z (vertical), where no friction resistance on supports is assumed (left upper panel). The corresponding strain (right upper panel). The lower figures show the maximum value of the cable tension without and with friction resistance and the elastic lengthening of the cable computed in zeroth order, respectively.*

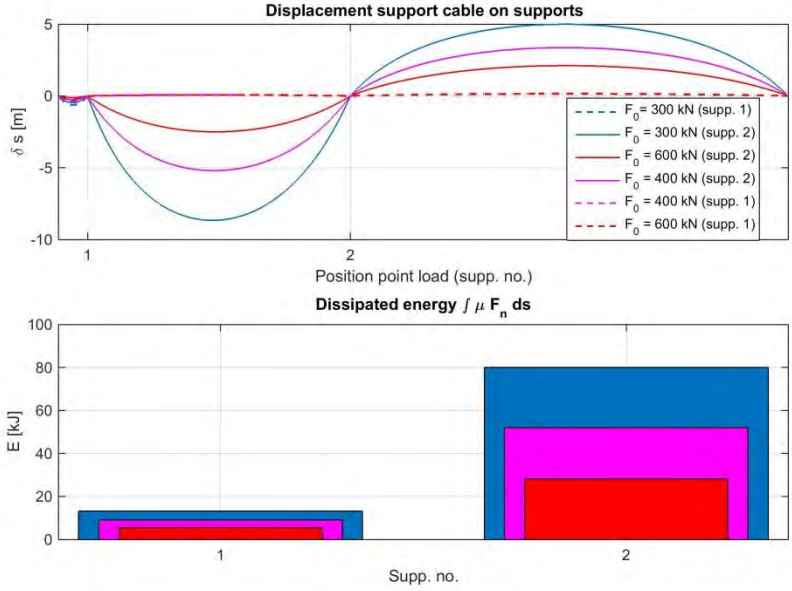

Fig. 3: *Ideal gliding support cable on the towers for different cable tensions F_0 at fixed temperature T_{curr} = 25* °C*. A negative value for δs means that the cable moves to the left (valley side). The data can help to estimate the possibility to bring the cable outside the support range for inspection using a sufficient point load. The lower part shows the heat production due to friction resistance during the ride, where the*

dynamic friction coefficient is μ=0.1 (colors corresponding to the upper plot). The heat production at the first support is quite smaller than at the second one because the small displacement of the cable. Exists a relationship between dissipated energy and cable material consumption?}

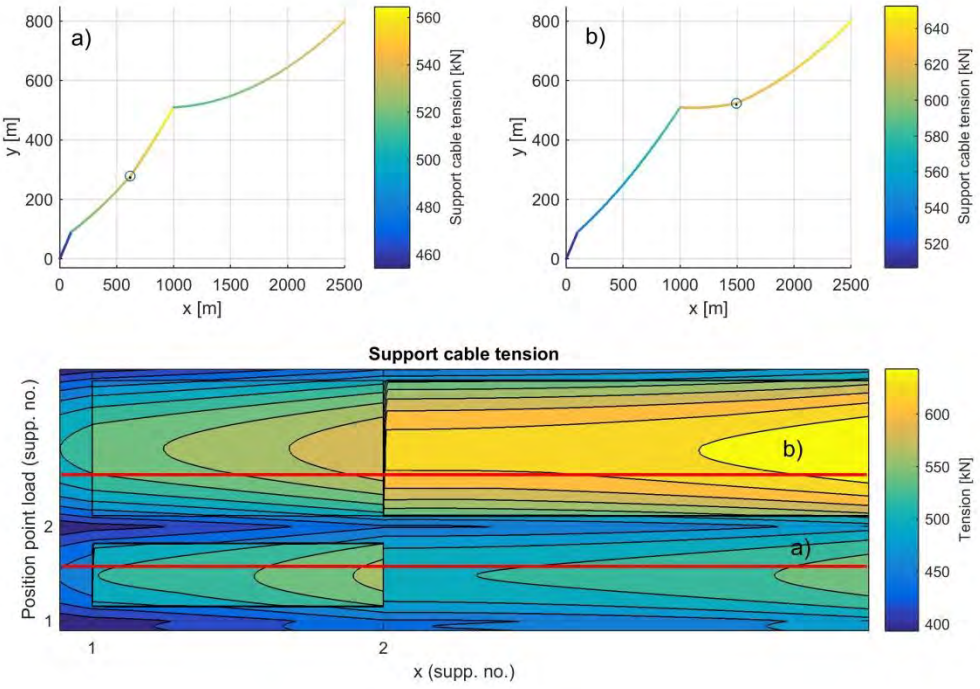

Fig. 4: *Tension of the support cable at T = 25 °C for two different positions of the point load (circles) over the whole line. In a) the point load is near the middle of the second span, in b) in the third span respectively. The presence of the friction resistance on the towers is clearly visible. The lower part shows the cable tension landscape for all positions of the point load and all cable positions including friction resistances. This contour plot answers to the question, how great is the tension at the position x, when the point load is at the position x_Z. The upper situations are indicated by red lines.*

Oscillations of point loads and cables

An important issue is the simulation of unwanted oscillations of the car and the cables [9-15]. Using the quasi-static approach, we can solve immediately one of the many problems, namely the computation of the ``spring constant'' k for vertical oscillations as a function of the position. Strictly spoken k is not a constant and the oscillations are not pure harmonic, but a Fourier synthesis is required. In Fig. 5 we have plotted k for three different masses as a function of point load position x_Z, where k is computed simply by the difference of force (i.e. the weight of the point load) divided by the difference of catenary sag (i.e. charged cable and empty cable). We should remark that in this computation the action of the hauling cable was included. For a first approximation this approach is sufficient. If we take into account various other effects, in frictions, the obtained results change significantly.

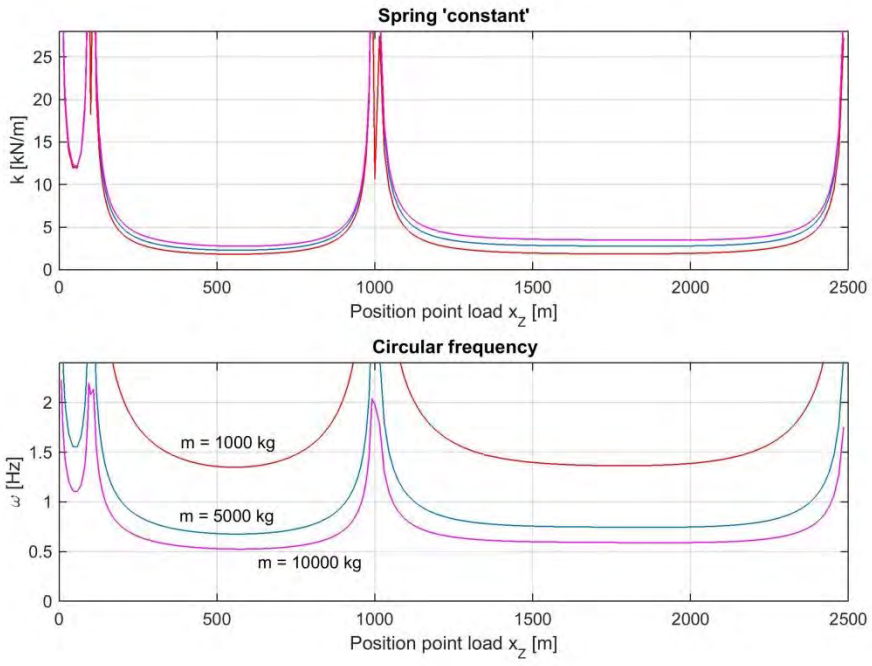

Fig. 5: *The computation of the static span catenary sag allows the determination of the (non-constant) ``spring constant'' k for the vertical displacement of a point mass sitting at position x_Z. As the relation force-displacement is non-linear, the different lines for different masses does not coincide (upper figure). Near the supports k becomes bigger, as expectable from intuition. The lower plot shows the corresponding angular frequency* $\omega = \sqrt{k/m}$. *The values of k and ω close to and at the supports are not relevant, because there the space extension of the towers are not negligible and also other effects become important.*

Outlook

A complete simulation of a ropeway leads to a large number of quantities. In this review we have presented only a few, a realistic standard simulation takes into account also the mountain profile and the hauling cable.

Further environmental conditions as wind and snow are of importance, the dynamical behavior (oscillations) and the peak power as well as the power consumption of the electrical engine are of interest.

This makes the parameter space of a possible ropeway plant extremely large and discontinuous. If a robust and fast computer program is available, which allows parallel computing on a cluster, a large class of different models can be simultaneously simulate and supposed a quality criterion has been established, the best of all can be extracted. The mathematical theory of optimization is working on such inverse problems, and the application to ropeway planning is still a wide open research field [16, 17].

Acknowledgment

The authors wish to acknowledge the Amt für Innovation, Forschung und Universität der Autonomen Provinz Bozen for financial support. This work is a part of the project ``Development of a simulation tool for cable railway oscillations''.

Author adresses

M. Wenin, CPE Computational Physics and Engineering, Weingartnerstrasse 28, 39011 Lana, BZ, Italy

M. Irschara, I&M Ingenieure, Kapuzinerplatz 9, 39031 Bruneck, BZ, Italy

S. Obexer, Ropes GmbH, Staatstr. 15, 39030 Vintl, BZ, Italy

M. L. Bertotti and G. Modanese, Free University of Bozen/Bolzano, Piazza Universit_a 1, 39100 Bolzano, BZ, Italy

Bibliography

[1] Matlab homepage https://de.mathworks.com/products/matlab.html, accessed: 2017-03-16.

[2] H. Göldner, J. Altenbach, H. Bergander, K. Eschke, R. Kreissig, and G. Landgraf, Höhere Festigkeitslehre (Band 2) (Physik-Verlag Weinheim, 1985).

[3] R. Beha, Bewegungsverhalten und Kraftwirkungen des Zugseiles und der Fahrzeuge von Zweiseilbahnen zur Berechnung der Dynamik des Gesamtsystems (Dissertation) (Institut für Fördertechnik der Universität Stuttgart, 1994).

[4] S. Liedl, Bewegungen und Kräfte des Seilsystems und der Fahrzeuge von Seilschwebebahnen im Fahrbetrieb (Dissertation) (Herbert Utz Verlag, 1999).

[5] Mathematica homepage, https://www.wolfram.com/mathematica/, accessed: 2017-03-16.

[6] The sonification handbook, http://sonification.de/handbook, accessed: 2017-03-16.

[7] E. Czitary, Seilschwebebahnen (2. Auage) (Springer Verlag Wien, 1962).

[8] CEN-Norm, Sicherheitsanforderungen für Seilbahnen für den Personenverkehr (Amtsblatt der EU C51, 2009).

[9] E. Engel und R. Löscher, Arbeiten des Institutes für Eisenbahnwesen, Verkehrswirtschaft und Seilbahnen / eiba.tuwien.ac.at/_leadmin/mediapool-eisenbahn/Diverse/Institutshefte/ih31.pdf (2003).

[10] M. Volmer, Stochastische Schwingungen an ausgedehnten Seilfeldern und ihre Anwendung zur Spurweitenberechnung an Seilbahnen (Dissertation ETH Nr. 13379, 1999).

[11] G. Kopanakis, Internationale Seilbahn-Rundschau 1,22 (2010).

[12] D. Bryja and M. Knawa, Computers and Structures 98,1895-1905 (2011).

[13] J. A. Wickert and C. D. Mote, Journal of Sound and Vibration 149(2),267-284 (1991).

[14] X. Zhou, S. Yan, and F. Chu, Journal of Sound and Vibration 133 031001 (2011).

[15] H. M. Irvine and T. K. Caughey, Proc. R. Soc. London A 341, 299-315 (1974).

[16] H. Thaler, M. Wenin, J. Brunner, D. Reiterer, M. L. Bertotti, G. Modanese, and E. Oberhuber, Advanced Structured
Materials (Springer), pp 113-124 (2016).

[17] D. Pataria, Problems of mechanics, ISSN 1512-0740 / N 2(31) (2008).